Insect Biochemistry and Molecular Biology 105 (2019) 43–50

Contents lists available at ScienceDirect

Insect Biochemistry and Molecular Biology

journal homepage: www.elsevier.com/locate/ibmb

Identification of a novel function of the silkworm integument in nitrogen metabolism: Uric acid is synthesized within the epidermal cells in *B. mori*

Tsuguru Fujii*, Yutaka Banno

Laboratory of Silkworm Genetic Resources, Institute of Genetic Resources, Graduate School of io Resources and Bioenvironmental Science, Kyushu University, Fukuoka, 819-0395, Japan

ARTICLE INFO

Keywords:
Nitrogen metabolism
Pigmentation
Uric acid
Xanthine dehydrogenase
Molybdenum cofactor
Mosaic analysis

ABSTRACT

During nitrogen metabolism, animals convert toxic ammonia to less toxic forms. Uric acid (UA) is an end product of this process in terrestrial insects. In lepidopteran larvae, a large amount of UA is stored in the integument via a phenomenon known as storage excretion. Physiologically, integumental UA plays crucial roles as a barrier against sunlight and as a white pigment for larval pigmentation patterns. Conventionally, UA is thought to be synthesized in the fat body, the insect equivalent of the liver of vertebrates, and to be transported to the epidermis via the hemolymph. Here, we reconsidered the conventional theory by a mosaic analysis targeting genes governing UA synthesis, using CRISPR/Cas9 mutagenesis and a traditional genetic method in *Bombyx mori*. Notably, we observed mosaic larvae in which the integument comprised both UA-containing white and UA-lacking translucent areas, indicating that UA synthesis in the epidermis is indispensable to the accumulation of a large amount of highly insoluble UA in the epidermis. Our results thus provide a genetic basis for storage excretion wherein lepidopteran insects use nitrogenous waste to adapt to their environment.

1. Introduction

Lepidopteran larvae are herbivorous, feeding on plants leaves. The order Lepidoptera is the second-largest group among insects that have diversified by adapting to various host plants. Plants depend on sunlight for photosynthesis; however, sunlight is harmful to animals because cell DNA is damaged by ultraviolet radiation (Ichihashi et al., 2003; Cadet et al., 2005). Moreover, lepidopteran larvae on leaves are easily found by parasitoids, wasps, and birds compared with insects that live underground. Therefore, larval pigmentation pattern is an important trait for lepidopteran insects as a means of barrier against sunlight and to make their body camouflaged from enemies (Matsuo and Ishikawa, 1999; Greeney et al., 2012; Hu et al., 2013). Elucidation of the molecular mechanism controlling larval pigmentation patterns will help understand how lepidopteran insects have diversified by adapting to their habitats.

Detoxification and excretion of toxic metabolites are essential processes in animals. For example, mammals convert ammonia, a toxic byproduct of the catabolism of nitrogen-rich compounds (e.g., amino acids and purines), to the less toxic urea, which can be diluted in water and excreted. In terrestrial insects, uric acid (UA) is a major excretory nitrogenous waste product (O'Donnell, 2008), and its low solubility enables insects to excrete UA in a crystallized form, which conserves water required for excretion. Moreover, UA can be stored within the body without affecting homeostasis via a phenomenon known as storage excretion. Insects particularly require storage excretion during various stages of their life cycle (e.g., embryogenesis and pupal stage) when excretion of nitrogenous waste is impossible (Wigglesworth, 1972).

Insects excrete UA through Malpighian tubules, which discharge into the intestine (Wigglesworth, 1972). Even when Malpighian tubules are functional, some insects exhibit storage excretion. Specifically, lepidopteran species, such as *Bombyx mori*, *Manduca sexta*, *Pieris brassicae*, and *Papilio polyxenes*, accumulate large amounts of UA in the larval epidermis which is the thin layer of cells beneath the thick cuticle in the integument (Lhonoré et al., 1980; Buckner and Newman, 1990; Tamura and Akai, 1999; Timmerman and Berenbaum, 1999). In the lepidopteran larva, UA has multiple roles: (i) it shields the larval body from ultraviolet radiation from the sun (ii) it acts as a scavenger of photo-induced reactive oxygen species (Matsuo et al., 1999; Hu et al., 2013) and (iii) it is used as a white pigment to form the larval pigmentation pattern (Lhonoré et al., 1980; Buckner and Newman, 1990; Timmerman and Berenbaum, 1999; Tamura and Akai, 1999). For example, the integument of the third-instar larvae of *P. polyxenes* resembles a bird dropping because it comprises black and white areas with low and high UA contents, respectively (Timmerman and

* Corresponding author.
E-mail address: fujii.tsuguru.233@m.kyushu-u.ac.jp (T. Fujii).

https://doi.org/10.1016/j.ibmb.2018.12.014
Received 15 September 2018; Received in revised form 28 December 2018; Accepted 28 December 2018
Available online 02 January 2019
0965-1748/

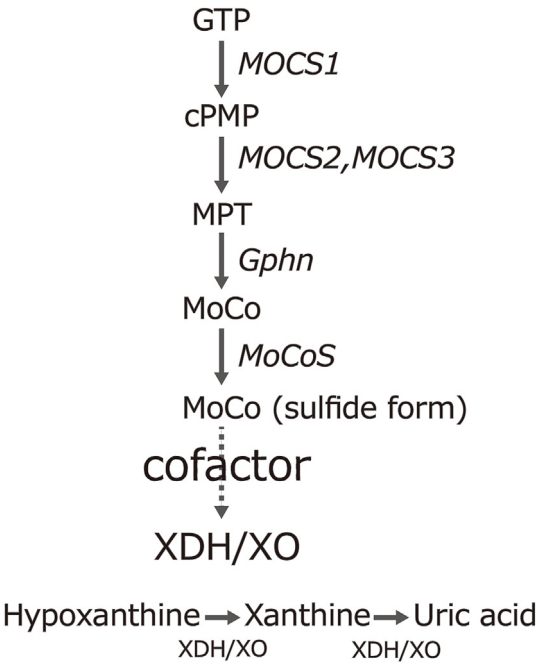

Fig. 1. Molybdenum cofactor (MoCo) biosynthetic pathway. GTP: guanosine triphosphate; cPMP: cyclic pyranopterin monophosphate; MPT: molybdopterin; *MOCS1*, *2*, and *3*: molybdenum cofactor synthesis-step 1, 2, and 3 genes, respectively; *Gphn*: gephyrin gene; *MoCoS*: MoCo sulfurase gene; XDH: xanthine dehydrogenase; XO: xanthine oxidase.

Berenbaum, 1999). In *B. mori*, UA accumulates in granules to yield a white color and opaqueness to the larval integument; consequently, lack of UA granules causes a translucent larval integument (Tamura and Akai, 1999). *B. mori* is rich in translucent mutants that have been classified into two types: a type that cannot synthesize UA and the other that cannot accumulate UA in the epidermis (Tamura and Sakate, 1983; Tamura and Akai, 1999). *B. mori* larvae which devoid of UA in their integument is sensitive to the UV damage (Matsuo and Ishikawa, 1999; Hu et al., 2013).

Xanthine dehydrogenase (XDH) is a key enzyme in UA synthesis (Fig. 1). In an evaluation of various tissues of *B. mori*, it was observed that the fat body, the insect equivalent of the liver of vertebrates, had the highest level of XDH activity, whereas the integument lacked such an activity (Hayashi, 1960), thus indicating that UA is synthesized in the fat body, released into the hemolymph, and transported to the epidermis. Subsequent experiments involving injection of ^{14}C-labeled UA into *B. mori* and *M. sexta* larvae confirmed that UA is transported via the hemolymph and accumulates in the epidermis (Tamura and Sakate, 1983; Buckner and Newman, 1990). Despite the long history of research on storage excretion in Lepidoptera, it remains unknown how large quantities of insoluble UA are transported to the *B. mori* larval epidermis.

XDH activity depends on the sulfide form of molybdenum cofactor (MoCo) (Fig. 1) (Schwarz et al., 2009). In *B. mori*, the *og* locus encodes MoCo sulfurase (MoCoS), which is required for MoCo sulfuration (Kômoto et al., 2003). Accordingly, XDH activity is abolished in *og* mutants, in which the larval integument lacks UA and is translucent (Tamura, 1977). Mutants lacking XDH activity are poorly viable after pupation and must be maintained via crosses of normal moths with the mutant alleles in a heterozygous state. og^z is a null mutation allele in the *Bombyx MoCoS* gene (*BmMoCoS*) (Fujii et al., 2009). During this process of og^z allele maintenance, we happened to observe a mosaic larva comprising both a translucent and opaque integument. Because mosaic larvae can be generated via gene mutation, chromosomal aberration, and unusual fertilization modes (Tazima, 1964), we presumed that the opaque and translucent areas of the mosaic larval integument reflected the wild-type and og^z genotypes, respectively. Occurrences of mosaicism have been reported to arise from translucent mutant loci such as *od*, *oa*, and *w-3* which governs the accumulation of UA in the epidermis (Fujii et al., 2010, 2012; Fujii and Banno, 2018; Kômoto et al., 2009; Ando and Fujiwara, 2013). However, if UA is synthesized in the fat body and transported via the hemolymph to accumulate in the epidermis, mosaicism of the integumental translucency would not occur in translucent mutants lacking XDH activity. This accidental finding of the mosaic larva in the og^z strain led us to conduct mosaic analysis targeting genes controlling UA synthesis in *B. mori*.

Here, we report an experimental generation of mosaic larvae with opaque and translucent integument through mosaic analysis of genes governing synthesis of UA, including *BmXDH1*, *Bombyx Gephyrin* (*BmGphn*), and *BmMoCoS*. *BmXDH1* encodes the protein with major XDH activity, *BmGphn* is indispensable for MoCo synthesis, and *BmMoCoS* governs MoCo sulfuration. Previously, we reported that the dual sgRNA strategy developed for butterfly species was applicable to CRISPR/Cas9 genome editing in *B. mori* (Fujii et al., 2018; Fujii and Banno, 2018). Knockout efficiency of this methods is very high and knockout phenotypes such as mosaicism or targeted gene null phenotype can be observed in an sgRNA/Cas9 injected generation (Zhang and Reed, 2016, 2017; Fujii and Banno, 2018). Mosaicism of *BmXDH1* and *BmGphn* was induced by the dual sgRNA strategy, whereas that of *BmMoCoS* was induced by introducing the *mo* mutation into a strain with og^z mutation. The *mo* mutation causes the generation of mosaic larvae via the frequent non-elimination of polar bodies during meiosis and subsequent double fertilization events (Ebinuma et al., 1988; Fujii et al., 2011). Our results indicate that synthesis of UA in significant quantities and synthesis and sulfuration of MoCo occur in the larval epidermis.

2. Materials and methods

2.1. Silkworm strains

The four *B. mori* strains used in this study, p50, p55, o35, and o36, are stocked at Kyushu University with partial support from the National BioResource Project. The o35 and o36 strains have been maintained using $+/og^t$ and $+/og^z$ moths, respectively. Phenotypically, homozygotes of og^t and og^z have a translucent integument due to a lack of XDH activity (Tamura, 1977; Kômoto et al., 2003; Fujii et al., 2009). A strain harboring the *mo* mutation was kindly provided by Dr. Hiroaki Abe (Tokyo University of Agriculture and Technology). Homozygotes for the *mo* mutation generate mosaic larvae via the frequent non-elimination of polar bodies during meiosis and subsequent double fertilization events (Ebinuma et al., 1988; Fujii et al., 2011). The p55 and p50 strain is a standard non-diapause and diapause strain for which the genome has been sequenced (silkbase; http://silkbase.ab.a.u-tokyo.ac.jp), respectively. Non-diapause eggs laid by p55 females crossed with p50 males were used for CRISPR/Cas9 genome editing of *BmXDH1* while non-diapause eggs laid by p55 females crossed with p55 males were used for that of *BmGphn*.

2.2. Genomic PCR, reverse transcription-PCR, and cloning

Genomic DNA was extracted from moths using the DNeasy Blood and Tissue Kit (Qiagen, Valencia, CA, United States). Total RNA was prepared from the tissues (fat body, epidermis, hemocyte, Malpighian tubule, and midgut) of the day-3 fifth instar larvae using RNAiso (TaKaRa Bio, Otsu, Shiga, Japan). First-strand cDNA was synthesized from 1 μg of total RNA using the PrimeScript™ II 1st strand cDNA Synthesis Kit (TaKaRa Bio) with an oligo dT primer. Genomic PCR was performed using ExTaq (TaKaRa Bio) while RT-PCR was performed with KOD FX Neo (Toyobo, Osaka, Japan). See Table S1 for the primer sets designed to amplify the *BmXDH1, BmMOCS1, and BmGphn* sequences. The primer set used to amplify the *BmMoCoS* sequence were

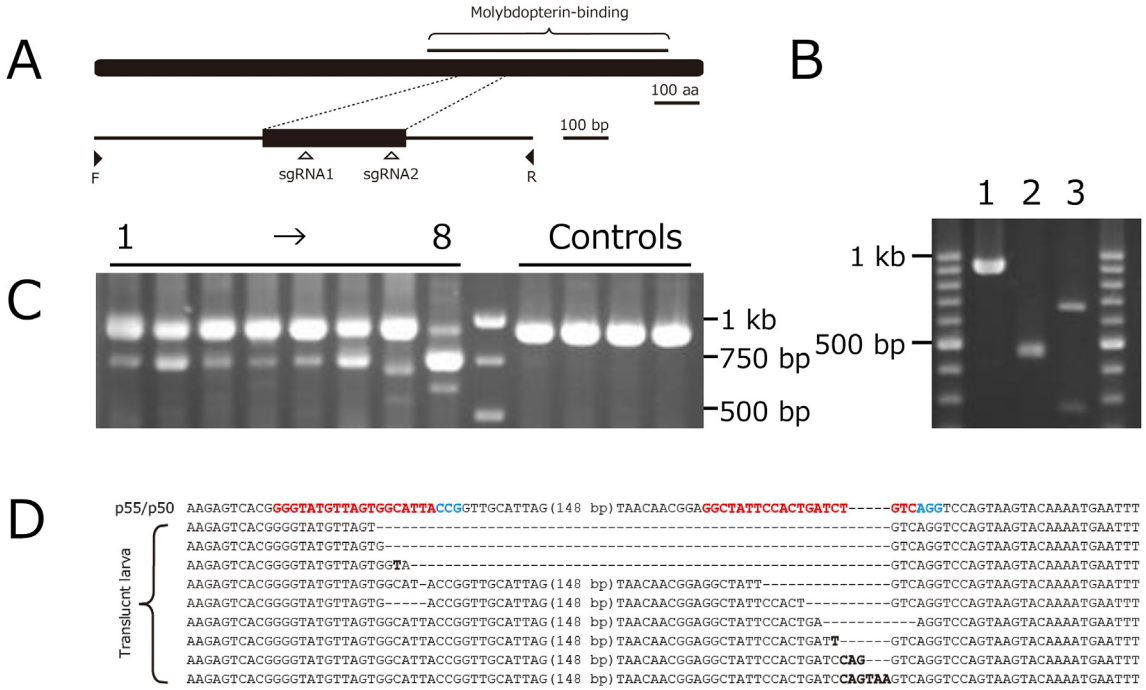

Fig. 2. PCR and sequencing analysis of CRISPR/Cas9-mediated mutations in *BmXDH1*. (A) Location of the sgRNAs and primers relative to the *BmXDH1* gene. F and R indicate the primers used to amplify the sequence containing the sgRNA target sites. (B) Analysis of the cleavage products. Lane 1, Untreated target fragment. Lane 2 and 3, Target fragments treated with the Cas9/sgRNA1 mixture (lane 2) and the Cas9/sgRNA2 mixture (lane 3). (C) Eight randomly selected translucent larvae segregated in the G_0 generation were subjected to PCR analysis to amplify the region containing the two target sites of the sgRNAs. The primer set shown in Fig. 2A was used. Four F_1 individuals obtained by crossing p55 females to p50 males were used as controls. (D) Alignment of *BmXDH1* sequences cloned from a control (p55/p50) and translucent individual in Fig. 2C. The substituted sequences are indicated in bold. Blue: sgRNA targets. Red: PAM sequences. (For interpretation of the references to color in this figure legend, the reader is referred to the Web version of this article.)

previously described (Fujii et al., 2009). *BmRpL3* was used as a positive control for RT-PCR. The primers used for *BmRpL3* were previously described (Sato et al., 2008). The primer sets used in RT-PCR analysis span introns of each gene, which makes it possible to distinguish target products from false positives amplified from genomic DNA which may contaminate the cDNA. PCR products were cloned into pGEM-T easy vectors (Promega Corp., Madison, WI, United States) and sequenced via BigDye terminator cycle sequencing (Applied Biosystems, Foster City, CA, United States).

2.3. CRISPR/Cas9 genome editing

For the genome editing experiment, sgRNAs were designed according to the dual sgRNA strategy (Zhang and Reed, 2016, 2017). Two sgRNAs were designed for the target gene, *BmXDH1*, by using CRISPRdirect (https://crispr.dbcls.jp/) (Naito et al., 2015). We confirmed that the designed sgRNAs should not cause off-target effects by performing the off-target search. The cleavage efficiency of sgRNAs was assayed using the Guide-it™ sgRNA In Vitro Transcription and Screening System (TaKaRa Bio) (Fig. 2A and B). For the genome editing of *BmGphn*, two sgRNAs reported in our previous manuscript were used (Fujii et al., 2018). Recombinant Cas9 protein was purchased from TaKaRa Bio (catalog number: Z2641N). PCR templates for the in vitro transcription of the two sgRNAs were synthesized according to the manufacturer's instructions, using two forward primers (CRISPR-1F and CRISPR-2F) and a common reverse primer. PCR products containing the sgRNA target sites were amplified using the primer set CUT-F/CUT-R (Fig. 2A). The cleavage efficiencies of the sgRNAs were evaluated in vitro by mixing Cas9 protein, a PCR product containing the target sites, and a designed sgRNA according to the manufacturer's instructions (Fig. 2B). The PCR primers used in this study are shown in Table S1. We mixed 1 μg of Cas9 protein and 375 ng of each sgRNA in a 5-μL volume prior to injection as described previously (Fujii et al., 2018; Fujii and Banno, 2018; Zhang and Reed, 2016, 2017). For the genome editing of *BmGphn,* the volume of Cas9 protein was doubled in the Cas9/sgRNA mixture. The Cas9/sgRNA mixtures were injected into freshly laid (i.e., within 4 h) eggs.

2.4. Injection of bovine xanthine oxidase and quantification of UA content in the larval integument

MoCo-containing XO (0.3 U/mg protein) purified from bovine buttermilk was purchased from Oriental Yeast Co., Ltd. (Tokyo, Japan). A de novo supply of MoCo is not needed to induce the activity of MoCo-containing XO (Tamura et al., 1999; Fujii et al., 2016). The XO solution was prepared by dissolving the enzyme in Grace insect medium as described previously (Tamura et al., 1999; Fujii et al., 2016). Subsequently, 20 μL (0.1 mg/μL) of the solution was injected into day-1 fifth-instar larvae through a leg. The subjects were observed and dissected two days later. Injection was conducted once per individual. The UA contents of the larval integuments were determined using a Uric Acid C-test Wako (Wako Pure Chemical, Chuo-ku, Osaka, Japan) as described previously (Tamura et al., 1999; Fujii et al., 2016). We mixed 3 mL of Uric acid assay buffer and 50 μL of a uric acid samples prepared by larval integument following the manufacture's introduction. We then measured the OD of the mixed solution at 555 nm using a 3 mL cuvette with the SP-808 spectrophotometer (T and T Co., Ltd) and the uric acid content of the sample was colorimetrically determined.

3. Results

3.1. mRNA expression of genes governing UA synthesis

XDH is a key enzyme in the catalysis of hypoxanthine to xanthine and xanthine to UA. XDH activity depends on the sulfurated form of MoCo (Fig. 1). In *B. mori*, *BmXDH1* encodes the protein with major XDH

activity and *BmMoCoS* governs the sulfuration of MoCo (Kômoto et al., 1999, 2003; Kômoto, 2002). In eukaryotes, MoCo is synthesized by a conserved biosynthesis pathway governed by four loci: *MOCS1, MOCS2*, *MOCS3*, and *Gphn* (Fig. 1) (Schwarz, 2009). The *Bombyx* ortholog of *MOCS1* and *Gphn* have been genetically characterized and were found to govern the synthesis of MoCo (Fujii et al., 2016, 2018). It was reported that the XDH activity of the fat body was found to be much higher than that in the other larval tissues, and activity was also detected in the Malpighian tube and mid gut, but not in the integument and hemolymph (Hayashi, 1960: 1961). However, a library of full-length cDNAs from epidermal samples contains *BmXDH1* (Okamoto et al., 2009), and RNA-seq data from the epidermises of *B. mori* indicate that *BmMOCS1*, *BmGphn*, *BmMoCoS* and *BmXDH1* are expressed in the larval epidermis (Zhang et al., 2017). To confirm the expression of these four genes in the epidermis, RT-PCR analysis was performed in a standard *B. mori* strain (p50). Amplification products were obtained from every gene in the epidermis as observed in the other tissues (fat body, mid gut, Malpighian tube, and hemocyte) (Fig. S1), suggesting that UA is synthesized in a variety of tissues other than the fat body.

3.2. Mosaic analysis targeting BmXDH1

To determine whether UA is synthesized in the epidermis, we used CRISPR/Cas9 mutagenesis targeting *BmXDH1*, which encodes the protein with major XDH activity (Kômoto et al., 1999; Kômoto, 2002). We designed two sgRNAs to target the molybdopterin-binding domain of *BmXDH1*, because truncation of this domain abrogates the activity of BmXDH1 (Kômoto, 2002) (Fig. 2A). We mixed Cas9 protein with the two sgRNAs and injected the mixture into freshly laid eggs, as described previously (Zhang and Reed, 2016, 2017). Subsequently, during the fifth instar stage, the larvae exhibited translucent, intermediately translucent, or mosaic appearances (i.e., translucent and opaque integuments) (Fig. 3; Table 1).

To confirm that the *BmXDH1* mutation caused the translucent phenotype, eight randomly selected translucent individuals were subjected to PCR analysis. DNA from all individuals yielded a smaller band (length: ~750 bp) that was absent in the PCR products amplified from controls (Fig. 2C). Two PCR products (~750 bp and 1 kb in length) from a translucent individual were then sequenced (Fig. 2D). Here, long deletions spanning the two sgRNA target sites were identified in the former product, whereas short insertions/deletions in the vicinity of the target sites were identified in the latter. To further confirm that the translucent phenotype was caused by defective XDH activity, bovine XO was injected into the mosaic larvae. As XO shares a similar function with XDH, the injection of bovine XO caused the translucent integuments of the og^t and og^z larvae to become opaque [Tamura et al., 1999; Fujii et al., 2016]. In the absence of the XO injection, the mosaic phenotype did not change during the fifth instar stage (Fig. 4A and B). By contrast, the translucent integument became opaque two days after the injection, thus indicating that (i) this area of the integument lacked XDH activity, (ii) *BmXDH1* participated in UA synthesis in the epidermis, and (iii) the diffusion of BmXDH1 from a wild-type cell to the adjacent knockout cells was non-existent or limited (Fig. 4C and D).

Regarding the intermediately translucent larvae, the clear border between the translucent and opaque areas was not observed (Fig. 3B). To assess the difference between mosaic and intermediately translucent larvae, the epidermal UA contents were analyzed. Notably, the UA content was significantly lower in intermediately translucent larvae than normal larvae (Fig. 3E). These findings suggest that in intermediately translucent larvae, (i) the epidermis lacks XDH activity consequent to CRISPR/Cas9-mediated knockout of *BmXDH1* and (ii) the total amount of UA synthesized in the fat body and transported to the epidermis via the hemolymph is not enough to render complete integumental opaqueness due to the CRISPR/Cas9-mediated mosaicism of *BmXDH1* in the fat body.

3.3. Mosaic analysis targeting BmGphn

Mosaic analysis revealed that UA is synthesized in the epidermis by *BmXDH1* (Figs. 2–4; Table 1). XDH depends on sulfurated form of MoCo for its activity (Fig. 1). To assess whether MoCo is synthesized in the epidermis or transported via the hemolymph, we conducted mosaic analysis targeting *BmGphn*, which is one of the genes governing MoCo synthesis (Fig. 1).

We had previously obtained knockout alleles of *BmGphn* by applying the dual sgRNA strategy developed for butterfly species (Fujii

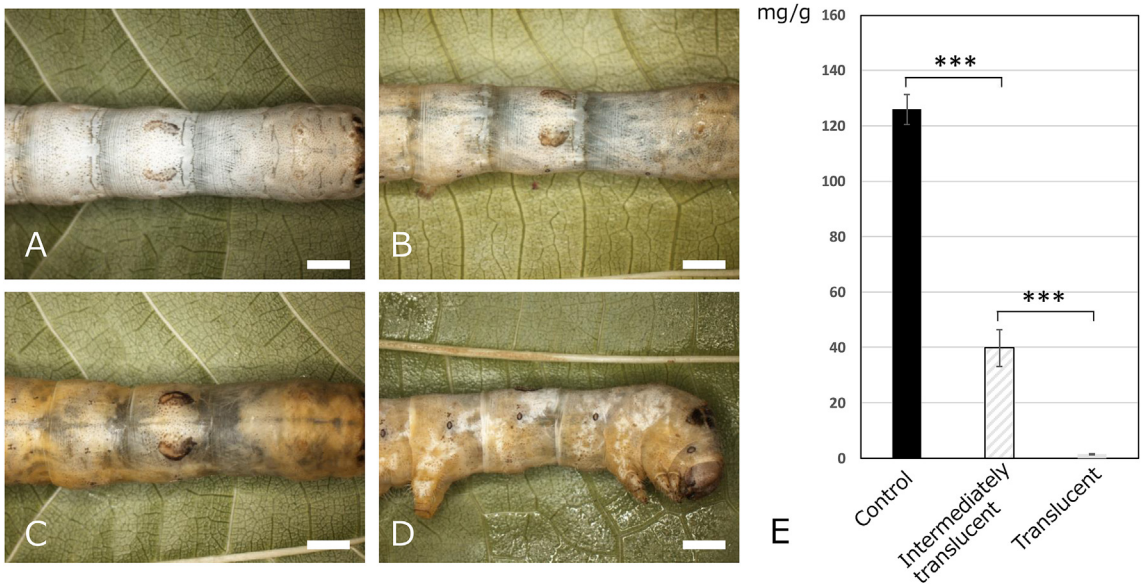

Fig. 3. Larval phenotype induced by the CRISPR/Cas9-mediated knockout of *BmXDH1*. (A) Control F_1 larva generated by crossing the p55 and p50 strains. (B) Intermediately translucent larva. (C) Translucent larva. (D) Mosaic larva. Bars = 3 mm. Larvae depicted in (B), (C), and (D) were obtained in the G_0 generation. (E) UA contents in the integuments of larvae induced by the CRISPR/Cas9-mediated knockout of *BmXDH1*. Control: Normal larvae obtained by crossing p55 females with p50 males (n = 5). Intermediately translucent larvae (n = 5). Translucent larvae (n = 5). Error bars represent s.d. ***$P < 0.001$, one-way analysis of variance with Tukey's multiple comparison post-test.

Table 1
Summary of the results from CRISPR/Cas9 injection experiment.

Target	Injected eggs	Larvae hatched	Larval phenotype observed in the fourth to fifth instar			
			Opaque	Intermediately translucent	Translucent	Mosaic
BmXDH1	672	363	0	19	103	22
BmGphn	144	66	4	2	18	7

Fig. 4. Effect of bovine XO injection on the translucency of mosaic larvae. (A) to (D) show the phenotypes of two CRISPR/Cas9-induced *BmXDH1* mosaic larvae obtained in the G_0 generation. The larva in (A) was injected with Grace insect medium, while the larva in (C) was injected with bovine XO. (B) and (D) respectively depict the phenotypes of these larvae 2 days after the indicated treatments.

et al., 2018; Zhang and Reed, 2016, 2017). Translucent integument, the knockout phenotype of *BmGphn,* was observed in the G_1 generations, but translucent and mosaic larvae were not observed in the G_0 generation; this may be attributed to the low cleavage efficiency of the two sgRNAs designed. For the mosaic analysis of *BmGphn,* we used these two sgRNAs but the Cas9 protein volume was doubled in the Cas9/sgRNA mixture.

We injected the Cas9/sgRNA mixture into freshly laid eggs and obtained translucent, intermediately translucent, and mosaic larvae, suggesting that increasing the Cas9 protein volume in the Cas9/sgRNA mixture improved the cleavage efficiency (Table 1, Fig. S2). The generation of mosaic larvae suggested the following: (i) *BmGphn* is involved in synthesis of MoCo in the larval epidermis, (ii) failure to synthesize MoCo in the larval epidermis leads to insufficient amount of UA that is required to render complete integumental opaqueness, and (iii) the diffusion of MoCo from a wild type cell to adjacent knockout cells was non-existent or limited. Similar to the *BmXDH1* knockout experiment, the generation of intermediately translucent larvae could be explained by mosaicism of *BmGphn*; in these larvae, we presumed the following: (i) the genotype of the larval epidermis is homozygous to the knockout alleles that prohibited synthesis of UA in the epidermis and (ii) the total amount of UA synthesized in the fat body and transported to the larval epidermis via the hemolymph is insufficient to render complete integumental opaqueness due to the mosaicism of *BmGphn* in the fat body.

3.4. Mosaic analysis targeting BmMoCoS

XDH activity depends on the sulfurated form of MoCo (Fig. 1) (Schwarz, 2009). The mosaic analysis targeting *BmXDH1* and *BmGphn* indicated that UA is synthesized in the larval epidermis using MoCo synthesized in the epidermis. This suggests that sulfuration of MoCo also occurs in the larval epidermis. To confirm it, we introduced the *mo* mutation into the o36 strain, which harbors the og^z, a null allele of *BmMoCoS* (Fujii et al., 2009). Homozygous *mo* females produce normal, mosaic, and polyploid offspring as a consequence of the frequent non-elimination of polar bodies during fertilization (Ebinuma et al., 1988; Fujii et al., 2011). Generally, CRISPR/Cas9 genome editing generates mosaic larvae in which small patches of wild type cells and knockout cells are distributed throughout the body, whereas the *mo* mutation often generates bilateral mosaic larvae. Dissection of wild type and mutant epidermis can be performed using bilateral mosaic larvae.

After crossing *mo/mo*, $og^z/+$ females with $og^z/+$ males, the phenotypes of the fifth instar larvae were observed. Notably, these included mosaic larvae in which the integument comprised both translucent and opaque areas (Fig. 5A; Table 2). Four experiments were then conducted to confirm that these mosaic larvae were produced by the og^z mutation. First, to exclude the possibility of other hidden translucent mutations in the o36 strain, *mo/mo*, $og^z/+$ females were crossed with independently maintained $og^t/+$ o35 males. Again, mosaic larvae were observed (Table 2). Second, *BmMoCoS* gene expression was analyzed in a mosaic larva via RT-PCR analysis of the RNA separately extracted from the translucent and opaque areas of the integument. As expected, *BmMoCoS* gene expression was not observed in the translucent area because og^z is the null mutation of the *BmMoCoS* gene (Fujii et al., 2009) (Fig. 5B and C). Third, bovine xanthine oxidase (XO) was injected into mosaic larvae, after which the phenotype was observed. We observed that the translucent areas of the mosaic larval integument became opaque within 2 days (Fig. 5D and E). Fourth, the UA content in the mosaic larval integument was measured (Fig. 5F). The UA contents markedly differed between the opaque and translucent areas, and this difference was attributed to the respective presence or absence of XDH activity in the epidermis. Taken together, we concluded that (i) the translucent areas of the mosaic larvae had a genotype of og^z/og^z or og^z/og^t; (ii) *BmMoCoS* contributes to the synthesis of the sulfide form of MoCo in the epidermis; (iii) larval epidermis can not synthesize enough amount of UA for complete integumental opaqueness if MoCo is not sulfurated in the epidermis; and (iv) in the wild-type cells, the diffusion of the sulfurated form of MoCo and the consequently activated BmXDH1 to adjacent cells does not occur or is limited.

Interestingly, compared with the non-mosaic opaque larvae, the mosaic larvae had markedly lower UA content in the opaque area. In contrast, the UA content in the translucent area was markedly higher in the mosaic larvae than in the non-mosaic translucent larvae (Fig. 5F). We presumed that in the mosaic larvae, mosaicism occurred in the fat body; therefore, UA synthesized in the wild-type fat body was transported to the epidermis via the hemolymph, thus leading to increased UA content in the translucent integument area. However, this fat body mosaicism also decreased the total amount of UA transported to the epidermis, thus leading to reduced UA content in the opaque integument area.

With respect to the observed intermediately translucent larvae (Table 2), RT-PCR analysis indicates that epidermis of intermediately translucent larvae is og^z homozygote (Fig. 5C). Similar to *BmXDH1 and BmGphn* knockout experiment, generation of intermediately translucent larvae can be explained by mosaicism of *BmMoCoS* (Table 2). Namely, in intermediately translucent larvae, we presumed that (i) UA was not

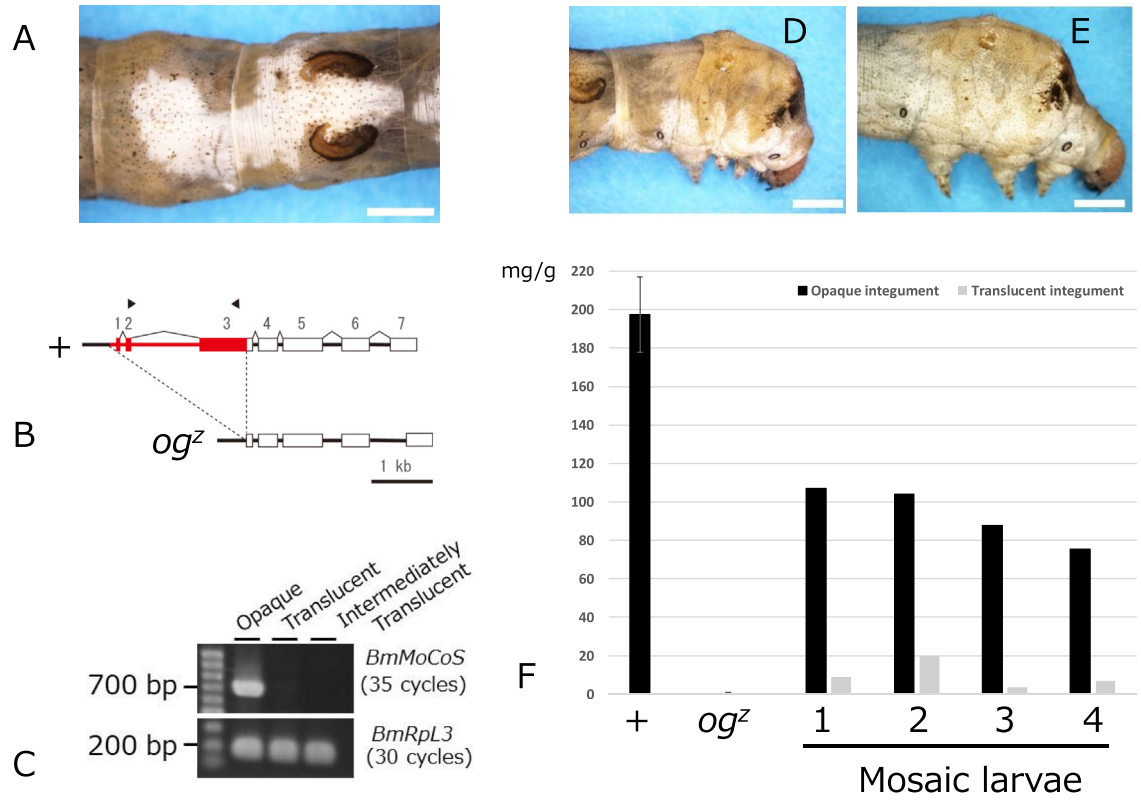

Fig. 5. Mosaic analysis of *BmMoCoS*. (A) A mosaic larva with opaque (+) and translucent (og^z) integument generated by the *mo* mutation. Bar = 3 mm. (B) Primers used for the RT-PCR analysis of *BmMoCoS*. The og^z allele lacks the red region which includes exons 1 and 2 and the 5′ part of exon 3 of the *BmMoCoS* gene (Fujii et al., 2009). (C) RT-PCR analysis of *BmMoCoS* in a mosaic larva and intermediately translucent larva generated using the *mo* mutation. RNA was extracted separately from the translucent and opaque areas of a mosaic larva. RNA was also extracted from the integument of an intermediately translucent larva. *BmRpL3* was used as a positive control. (D, E) Effect of bovine XO injection on the translucency of mosaic larvae. (D) and (E) demonstrate the phenotype of a *mo*-induced og^z mosaic larva before and 2 days after the XO injection, respectively. Bars = 3 mm. (F) UA contents in the larval integuments. +: Opaque larvae (n = 5). og^z: Translucent larvae (og^z/og^z) (n = 5). 1–4: Mosaic larvae with both opaque and translucent integument. The opaque and translucent areas of integument were dissected and independently subjected to UA analyses. Error bars represent s.d. (For interpretation of the references to color in this figure legend, the reader is referred to the Web version of this article.)

Table 2
Mosaic larvae and intermediately translucent larvae induced by the mo mutation.

Mating scheme	Batches reared	Larval phenotype observed in the fifth instar			
		Opaque	Translucent	Intermediately translucent	Mosaic
mo/mo, + /og^z × + /og^z	34	1817	467	5	60
mo/mo, + /og^z × + /og^t	2	267	51	0	4

Homozygous mo females produce mosaic larvae via the frequent non-elimination of polar bodies during meiosis and subsequent double fertilization event, irrespective of the mo genotype of the mated male (Ebinuma et al., 1988; Fujii et al., 2011).

synthesized in the epidermis (ii) the total amount of UA synthesized in the fat body and transported to the epidermis via the hemolymph is not enough to render complete integumental opaqueness due to the mosaicism of *BmMoCoS* in the fat body.

4. Discussion

During nitrogen metabolism in *B. mori*, toxic ammonia is first detoxified by converting it to glutamine (Hirayama and Nakamura, 2002). Ultimately, glutamine is converted to UA, which is excreted in feces or is accumulated in the larval epidermis via a phenomenon known as storage excretion (Wigglesworth, 1972; O'Donnell, 2008). In Lepidoptera, epidermal UA is physiologically very important because it protects the larval body from ultraviolet radiation from the sun and it acts as a white pigment to form larval pigmentation pattern (Lhonoré et al., 1980; Buckner and Newman, 1990; Matsuo and Ishikawa, 1999; Tamura and Akai, 1999; Timmerman and Berenbaum, 1999; Hu et al., 2013). As previously noted, XDH is a key enzyme in UA synthesis, and the distribution of enzymatic activity in the larval body has led to the conventional belief that UA is synthesized in the fat body and transported to the epidermis via the hemolymph (Hayashi, 1960). Subsequent molecular characterization of XDH has therefore focused on the fat body; accordingly, the lepidopteran integument has escaped detailed studies of XDH (Buckner et al., 1993; Kômoto et al., 1999; Kômoto, 2002). However, it remains unknown how large quantities of insoluble UA are transported to the epidermis.

Following our accidental finding of a mosaic larva with both the translucent and opaque integument from a strain with defective XDH activity, we suspected that the larval integument might be able to synthesize UA. To test this hypothesis, we conducted mosaic analyses targeting genes governing UA synthesis (*BmXDH1*, *BmGphn*, and *BmMoCoS*) using CRISPR/Cas9 mutagenesis and the *mo* mutation which generates bilateral mosaic larvae (Figs. 3 and 5; Fig. S2). Our findings from the mosaic larvae indicate the following: (i) *BmXDH1* is involved in the synthesis of significant quantities of UA in the larval epidermis (Fig. 4), (ii) synthesis and sulfuration of MoCo occur in the larval epidermis (Fig. 5; Fig. S2), and (iii) the diffusion of the mono-oxo and sulfurated forms of MoCo and the consequently activated BmXDH1

from wild type cells to adjacent knockout cells was non-existent or limited in the larval epidermis (Figs. 3–5; Fig. S2). Our observation of intermediately translucent larvae in the mosaic analysis suggested that the epidermis lacked XDH activity in these larvae; accordingly, the total amount of UA transported to the epidermis via the hemolymph was not sufficient to render complete integumental opaqueness due to the mosaicism of targeted genes in the fat body (Fig. 3; Table 1). We conclude that mosaic larvae—those with opaque and translucent integuments—and intermediately translucent larvae are generated by mosaicism of the targeted genes (*BmXDH*, *BmGphn*, and *BmMoCoS*). The phenotypes are different because of differences in the spatial distribution of knockout cells within a larval body. Specifically, part of the epidermis retained XDH activity in the former while the epidermis lacked XDH activity, and some of the fat body cells retained it in the latter. Presumably, occurrences of intermediately translucent larvae are a common phenomenon observed in mosaic analysis targeting genes controlling XDH activity. However, we did not analyze the genotype of the fat body of the intermediately translucent larvae. Further studies are required for revealing the mechanisms of generation of the intermediately translucent larvae.

Genetic analysis of translucent mutants in *Bombyx mori* has led to the consideration of UA granules as lysosome-related organelles, similar to eye pigment granules in *Drosophila* (Fujii et al., 2010, 2012; Wang et al., 2013a; Zhang et al., 2017). In eye pigment granules, the surrounding membranes contain White and Scarlet transporters that dimerize to form functional transporters for brown pigment precursors (Ewart and Howells, 1998; Mackenzie et al., 2000). Similarly, the White/Brown complex controls the transport of red pigment precursors in the eyes (Ewart and Howells, 1998; Dreesen et al., 1988). Notably, XDH is synthesized in tissues outside of the compound eyes and transported to the eye pigment granules, and a mutation in the gene encoding XDH was shown to reduce the accumulation of red pigment in the eye pigment granules (Reaume et al., 1989, 1991). Altogether, XDH is responsible for the synthesis of the red pigment within the eye pigment granules in *Drosophila*. In *B. mori,* mutations in the gene encoding the White ortholog (BmWhite) and Brown paralog (Bmok) yield a translucent larval phenotype with decreased epidermal accumulation of UA (Kômoto et al., 2009; Wang et al., 2013b), thus suggesting that BmWhite and Bmok dimerize to regulate the transport of UA precursors, such as xanthine and hypoxanthine, in UA granules (Wang et al., 2013b). The similarities between UA and eye pigment granules suggest that BmXDH1 is responsible for UA synthesis within the former. Further, as noted in the previous section, the translucent phenotype can be rescued in larvae lacking XDH activity by injecting bovine XO (Tamura et al., 1999; Fujii et al., 2016). Two possible explanations have been suggested for this phenomenon: XO injection may increase the UA content in the hemolymph, thereby leading to the transportation of large quantities of UA to the epidermis; alternatively, the injected XO may be transported to UA granules, wherein it synthesizes UA as observed in eye pigment granules in *Drosophila*. Immunohistological experiments are warranted to elucidate the subcellular localization of BmXDH1 and the injected bovine XO.

Interestingly, *B. mori* larvae assimilate toxic ammonia into amino acids via the GS/GOGAT pathway, which is involved in silk protein synthesis (Hirayama and Namakura, 2002). Notably, the *B. mori* cocoon forms an important barrier that protects prepupae from sunlight (Daimon et al., 2010). As mentioned above, epidermal UA also serves a very important barrier function and contributes to larval pigmentation patterns (Lhonoré et al., 1980; Buckner and Newman, 1990; Timmerman and Berenbaum, 1999; Matsuo et al., 1999; Tamura and Akai, 1999; Hu et al., 2013). Both the assimilation of toxic ammonia in the silk gland and storage excretion of UA in the epidermis are examples of unique nitrogenous waste management systems that have evolved to allow Lepidopteran insects to adapt to the surrounding environment.

B. mori mutants that lack silk glands excrete large amounts of UA in feces, indicating that silk threads are a form of nitrogenous waste and that silk glands are important sites for nitrogen metabolism (Kobayashi et al., 1980). In insects, the fat body is thought to be the primary site for UA synthesis (O'Donnell, 2008; Wigglesworth, 1972). On the contrary, we revealed that significant quantities of UA can be synthesized in the larval epidermis in *B. mori*. In *B. mori* and *M. sexta*, part of the UA accumulated in the epidermis is translocated to the fat body before the wandering stage, thus indicating that the temporal movement of UA between the fat body and the epidermis is regulated by the endocrine system (Buckner and Newman, 1990; Tamura and Akai, 1999; Ehresmann et al., 1990; Toji, 1971). Further studies are warranted to clarify the physiological interactions between the three tissues (fat body, epidermis, and silk gland) for the detoxification of nitrogenous waste and the maintenance of high UA content in the epidermis.

In conclusion, our results indicate that UA accumulates in the epidermis via two pathways. In the first pathway (conventional), UA is transported to the epidermis via the hemolymph. In the second pathway (novel), UA is synthesized in the epidermis. The second pathway is indispensable to the accumulation of a large amount of UA, which is highly insoluble and is also difficult to transport in significant quantities via the hemolymph. To the best of our knowledge, our research is the first to reveal the role of the larval integument in the synthesis of UA in lepidopteran insects. Thus, our results provide a genetic basis for storage excretion wherein lepidopteran insects use nitrogenous waste as a white pigment with sun-shielding properties for larval pigmentation pattern.

Acknowledgements

The four *B. mori* strains (p50, p55, o35, and o36) were provided by the National Bioresource Project, Japan. We thank K Nishikawa, K Tamura, K Yamamoto, S Eguchi (Laboratory of Silkworm Genetic Resources, Institute of Genetic Resources, Graduate School of Bio Resources and Bioenvironmental Science, Kyushu University) for rearing silkworms. We are grateful to Dr. Y. Kaneko (Hirosaki University) for providing helpful discussions. This work was supported by JSPS (Japan Society for the Promotion of Science) KAKENHI (Grant-in-Aid for Young Scientists B (15K18810))

Appendix A. Supplementary data

Supplementary data to this article can be found online at https://doi.org/10.1016/j.ibmb.2018.12.014.

References

Ando, T., Fujiwara, H., 2013. Electroporation-mediated somatic transgenesis for rapid functional analysis in insects. Development 140, 454–458.
Buckner, J.S., Newman, S.M., 1990. Uric acid storage in the epidermal cells of *Manduca sexta*: localization and movement during the larval-pupal transformation. J. Insect Physiol. 36, 219–229.
Buckner, J.S., Otto, P.E., Newman, S.M., Graf, G., 1993. Xanthine dehydrogenase in the fat body of *Manduca sexta*: purification, characterization, subcellular localization and levels during the last larval instar. Insect Biochem. Mol. Biol. 23, 549–559.
Cadet, J., Sage, E., Douki, T., 2005. Ultraviolet radiation-mediated damage to cellular DNA. Mutat. Res. 571, 3–17.
Daimon, T., Hirayama, C., Kanai, M., Ruike, Y., Meng, Y., Kosegawa, E., Nakamura, M., Tsujimoto, G., Katsuma, S., Shimada, T., 2010. The silkworm *Green b* locus encodes a quercetin 5-O-glucosyltransferase that produces green cocoons with UV-shielding properties. Proc. Natl. Acad. Sci. U.S.A. 107, 11471–11476.
Dreesen, T.D., Johnson, D.H., Henikoff, S., 1988. The Brown protein of *Drosophila melanogaster* is similar to the White protein and to components of active transport complexes. Mol. Cell Biol. 8, 5206–5215.
Ebinuma, H., Kobayashi, M., Kobayashi, J., Shimada, T., Yoshitake, N., 1988. The detection of mosaics and polyploids in the hereditary mosaic strain of the silk moth, *Bombyx mori*, using egg colour mutants. Genet. Res. 51, 223–229.
Ehresmann, D.D., Buckner, J.S., Graf, G., 1990. Uric acid translocation from the fat body of *Manduca dexta* during the pupal-adult transformation: effects of 20-hydroxyecdysone. J. Insect Physiol. 36, 173–180.
Ewart, G.D., Howells, A.J., 1998. ABC transporters involved in transport of eye pigment precursors in *Drosophila melanogaster*. Methods Enzymol. 292, 213–224.

Fujii, T., Ozaki, M., Masamoto, T., Katsuma, S., Abe, H., Shimada, T., 2009. *A Bombyx mandarina* mutant exhibiting translucent larval skin is controlled by the molybdenum cofactor sulfurase gene. Genes Genet. Syst. 84, 147–152.
Fujii, T., Daimon, T., Uchino, Y., Banno, S., Katsuma, H., Sezutsu, T., Tamura, T., Shimada, T., 2010. Transgenic analysis of the *BmBLOS2* gene that governs the translucency of the larval integument of the silkworm, *Bombyx mori*. Insect Mol. Biol. 19, 659–667.
Fujii, T., Abe, H., Yamamoto, K., Katsuma, S., Shimada, T., 2011. Interspecies linkage analysis of *mo*, a *Bombyx mori* locus associated with mosaicism and gynandromorphism. Genetica 139, 1323–1329.
Fujii, T., Banno, Y., Abe, H., Katsuma, S., Shimada, T., 2012. A homolog of the human Hermansky-Pudluck Syndrome-5 (HPS5) gene is responsible for the *oa* larval translucent mutants in the silkworm, *Bombyx mori*. Genetica 140, 463–468.
Fujii, T., Yamamoto, K., Banno, Y., 2016. Molybdenum cofactor deficiency causes translucent integument, male-biased lethality, and flaccid paralysis in the silkworm *Bombyx mori*. Insect Biochem. Mol. Biol. 73, 20–26.
Fujii, T., Yamamoto, K., Banno, Y., 2018. Translucent larval integument and flaccid paralysis caused by genome editing in a gene governing molybdenum cofactor biosynthesis in *Bombyx mori*. Insect Biochem. Mol. Biol. 99, 11–16.
Fujii, T., Banno, Y., 2018. Enlargement of egg size by CRISPR/Cas9-mediated knockout of a sex-linked gene in the silkworm, *Bombyx mori*. J. Insect Biotechnol. Sericol. 87, 71–78.
Greeney, H.,F., Dyer, L.A., Smilanich, A.M., 2012. Feeding by lepidopteran larvae is dangerous: a review of caterpillars' chemical, physiological, morphological, and behavioral defenses against natural enemies. ISJ-Invert. Surviv. J. 9, 7–34.
Hayashi, Y., 1960. Xanthine dehydrogenase in the silkworm, *Bombyx mori* L. Nature 186, 1053–1054.
Hayashi, Y., 1961. Studies on the xanthine oxidase system in the silkworm, *Bombyx mori* L. (II) Some properties on the xanthine-oxidation by various tissue homogenates. J. Seric. Sci. Jpn. 30, 359–367 (in Japanese with English summary).
Hirayama, C., Nakamura, M., 2002. Regulation of glutamine metabolism during the development of *Bombyx mori* larvae. Biochim. Biophys. Acta 1571, 131–137.
Hu, Y.G., Shen, Y.H., Zhang, Z., Shi, G.Q., 2013. Melanin and urate act to prevent ultraviolet damage in the integument of the silkworm, *Bombyx mori*. Arch. Insect Biochem. Physiol. 83, 41–55.
Ichihashi, M., Ueda, M., Budiyanto, A., Bito, T., Oka, M., Fukunaga, M., et al., 2003. UV-induced skin damage. Toxicology 189, 21–39.
Kômoto, N., Quan, G.X., Sezutsu, H., Tamura, T., 2009. A single-base deletion in an ABC transporter gene causes white eyes, white eggs, and translucent larval skin in the silkworm *w-3(oe)* mutant. Insect Biochem. Mol. Biol. 39, 152–156.
Kômoto, N., Yukuhiro, K., Tamura, T., 1999. Structure and expression of tandemly duplicated xanthine dehydrogenase genes of the silkworm (*Bombyx mori*). Insect Mol. Biol. 8, 73–83.
Kômoto, N., 2002. A deleted portion of one of the two xanthine dehydrogenase genes causes translucent larval skin in the *oq* mutant of the silkworm (*Bombyx mori*). Insect Biochem. Mol. Biol. 32, 591–597.
Kômoto, N., Sezutsu, H., Yukuhiro, K., Banno, Y., Fujii, H., 2003. Mutations of the silkworm molybdenum cofactor sulfurase gene, *og*, cuse translucent larval skin. Insect Biochem. Mol. Biol. 33, 417–427.
Kobayashi, M., Hamano, K., Mukaiyama, F., 1980. Nitrogen economy of 5th-instar larvae of the *Nd* silkworm. J. Seric. Sci. Jpn. 49, 91–94 (in Japanese with English summary).
Lhonoré, J., Bouthier, A., Beydon, P., Pennetier, J.L., Lafont, R., 1980. The epidermalcell cycle during the last larval instar of *Pieris brassicae* (Lepidoptera). I. Cell ultrastructure and variations in pigment content. J. Comp. Physiol. B. 136, 11–22.
Mackenzie, S.M., Howells, A.J., Cox, G.B., Ewart, G.D., 2000. Sub-cellular localization of the White/Scarlet ABC transporter to pigment granule membranes within the compound eye of *Drosophila melanogaster*. Genetica 108, 239–252.
Matsuo, T., Ishikawa, Y., 1999. Protective role of uric acid against photooxidative stress in the silkworm, *Bombyx mori* (Lepidoptera : bombycidae). Appl. Entomol. Zool. 4, 481–484.
Naito, Y., Hino, K., Bono, H., Ui-Tei, K., 2015. CRISPRdirect: software for designing CRISPR/Cas guide RNA with reduced off-target sites. Bioinformatics 31, 1120–1123.
Okamoto, S., Futahashi, R., Kojima, T., Mita, K., Fujiwara, H., 2009. Catalogue of epidermal genes: genes expressed in the epidermis during larval molt of the *silkworm Bombyx mori*. BMC Genomics 9, 396.
O'Donnell, M., 2008. Insect excretory mechanisms. In: In: Simpson, S.J. (Ed.), Advances in Insect Physiology, vol. 35. Academic Press, Cambridge, MA, pp. 1–122.
Reaume, A.G., Clark, S.H., Chovnick, A., 1989. Xanthine dehydrogenase is transported to the *Drosophila* eye. Genetics 123, 503–509.
Reaume, A.G., Knecht, D.A., Chovnick, A., 1991. The *rosy* locus in *Drosophila* melanogaster: xanthine dehydrogenase and eye pigments. Genetics 129, 1099–1109.
Sato, K., Matsunaga, T.M., Futahashi, R., Kojima, T., Mita, K., Banno, Y., Fujiwara, H., 2008. Positional cloning of a Bombyx wingless locus flugellos (*fl*) reveals a crucial role for *fringe* that is specific for wing morphogenesis. Genetics 179, 875–885.
Schwarz, G., Mendel, R.R., Ribbe, M.W., 2009. Molybdenum cofactors, enzymes and pathways. Nature 460, 839–847.
Tamura, T., 1977. Deficiency in xanthine dehydrogenase activity in the *og* and og^t mutants of the silkworm, *Bombyx mori*. J. Seric. Sci. Jpn. 46, 113–119.
Tamura, T., Sakate, S., 1983. Relationship between expression of oily character and uric acid incorporation in the larval integument of various oily mutants of the silkworm. Bull. Seric. Exp. Stn. (Tokyo) 28, 719–740.
Tamura, T., Akai, H., 1999. Comparative ultrastructure of larval hypodermal cell in-normal and oily *Bombyx* mutants. Cytologia 55, 519–530.
Tamura, T., Kanada, T., Kômoto, N., Yukuhiro, K., Hasegawa, T., 1999. Rescue of *oq, og* and og^t mutants by injection of xanthine oxidase. J. Seric. Sci. Jpn. 68, 111–117.
Tazima, Y., 1964. Mosaicism. The Genetics of the Silkworm. Logos Press, London, pp. 146–164.
Timmerman, S., Berenbaum, M.R., 1999. Uric acid deposition in larva integument of black swallowtails and speculation on its possible functions. J. Lepid. Soc. 53, 104–107.
Tojo, S., 1971. Uric acid production in relation to protein metabolism in the silkworm, *Bombyx mori*, during pupal-adult development. Insect Biochem. 1, 249–263.
Wang, L., Kiuchi, T., Fujii, T., Daimon, T., Li, M., Banno, Y., Katsuma, S., Shimada, T., 2013a. Reduced expression of the dysbindin-like gene in the *Bombyx mori ov* mutant exhibiting mottled translucency of the larval skin. Genome 56, 101–108.
Wang, L., Kiuchi, T., Fujii, T., Daimon, T., Li, M., Banno, Y., Kikuta, S., Kikawada, T., Katsuma, S., Shimada, T., 2013b. Mutation of a novel ABC transporter gene is responsible for the failure to incorporate uric acid in the epidermis of *ok* mutants of the silkworm, *Bombyx mori*. Insect Biochem. Mol. Biol. 43, 562–571.
Wigglesworth, V.B., 1972. The Principles of Insect Physiology, seventh ed. Chapman and Hall, London.
Zhang, L., Reed, R.D., 2016. Genome editing in butterflies reveals that *spalt* promotes and *Distal-less* represses eyespot colour patterns. Nat. Commun. 7, 11769.
Zhang, H., Kiuchi, T., Wang, L., Kawamoto, M., Suzuki, Y., Sugano, S., Banno, Y., Katsuma, S., Shimada, T., 2017. *Bm-muted,* orthologous to mouse muted and encoding a subunit of the BLOC-1 complex, is responsible for the *otm* translucent mutation of the *silkworm Bombyx mori*. Gene 629, 92–100.
Zhang, L., Reed, R., 2017. A practical guide to CRISPR/Cas9 genome editing in Lepidoptera. In: Sekimura, T., Nijhout, H.F. (Eds.), Diversity and Evolution of Butterfly Wing Patterns: an Integrative Approach. Springer, Singapore.